

The Intercomparison of Mixed Nuclide Rod Source Sets Used to Calibrate Waste Assay Systems

J.M. Kirkpatrick, S. Philips, S. Croft
Canberra Industries Inc.
800 Research Parkway
Meriden, CT 06450
USA

ABSTRACT

The relative activities of five sets of commercially available, certified mixed-nuclide rod gamma sources have been measured. The results are compared with one another and with the manufacturer's calibration certificates in order to evaluate the self consistency, accuracies and uncertainties of the activities claimed. The comparison measurements were made with Canberra's Tomographic Gamma Scanner (TGS) System in Segmented Gamma Scanner (SGS) mode, operated with a single segment and using a 120% relative efficiency HPGe detector. Each set of six rods was measured in a rotating 208-liter drum geometry typical of applications in which such rod source sets are commonly used for both initial calibration and operational verification measurements. Three of the five source sets were found to be consistent with one another within the experimental and claimed certificate uncertainties; however, two of the mixed-nuclide source sets were found to have nuclide-to-nuclide variations of activity significantly in excess of expectations based upon the claimed 99% confidence-level uncertainties. Such discrepancies could introduce substantial bias into waste measurement results made using the afflicted rod sets as the calibration standards. The findings of this work lead us to conclude that, where possible, the certified activities and associated uncertainties on newly acquired sources should be independently confirmed before relying on them as calibration standards.

INTRODUCTION

Industry standards continue to push toward improved accuracy in waste measurements in order to reduce disposal and storage costs. These demands have resulted in the development of new and innovative assay technologies, such as the Segmented Gamma Scanning (SGS) and Tomographic Gamma Scanning (TGS) systems, with large volume Ge detectors, which are able to reduce systematic measurement uncertainties and therefore provide higher precision and accuracy measurement capabilities than traditional methods. With the advent of these new technologies, however, there comes an ever increasing reliance upon the accurate certification of calibration source standards, which will necessarily contribute increasing proportions of the total measurement uncertainty as other errors are reduced. With this in mind, a comparison study of five calibrated, mixed-nuclide rod sources from commercial manufacturers was recently performed at Canberra's Meriden, CT facility with the goal of evaluating the accuracy of the certificate activities claimed for each set.

DESCRIPTION OF MEASUREMENTS

While the absolute and independent verification of the certified activity of any one rod set presents considerable technical challenges, a relative comparison of the five sets of calibration standards is a comparatively easy measurement to perform and still provides sufficient information to make a collective, qualitative, and in some respects quantitative evaluation of the claimed accuracies of the source certificates. For the purposes of this comparative measurement, one rod set was selected to serve as a reference source and was used as a standard against which the other sets were measured. No presumption was made that this certificate reflects the true activity of the rod set. The activities obtained for each of

the other rod sets were then compared to the certificate values. If all of the source certificates were accurate to within the stated errors, we would expect all measured and certificate values to agree within the total combined experimental errors. As all of these measurements used the same methodology, apparatus, and geometry, any systematic experimental biases were canceled out in the final relative comparison.

Rod Source Sets

The nuclide contents of each of the five rod source sets are listed in Table 1. Each set is assigned a generic identifier, A – E, by which we will refer to them throughout this study. The certificate activities and uncertainties for each set are included in Appendix A. For each set of rod sources, the activities per nuclide of all six rods were summed to give a total activity for the set since this is the principal quantity tested in the present set-up.

Table I *Isotopic Mixes, Decay-Corrected Certificate Activities and Declared Uncertainties of Five Calibrated Rod Source Sets. The Activities and uncertainties represent the sum over six rods per set. The activities are given in μCi , and the relative statistical and systematic uncertainties indicate one standard deviation as a percent of the nominal activity. The total uncertainty is obtained from the sum, in quadrature, of the systematic and statistical uncertainties.*

Rod Set	Nuclide	Activity	Stat.	Syst.	Tot.
A	Am-241	32.756	0.15%	1.22%	1.23%
	Ba-133	22.973	0.15%	1.20%	1.21%
	Cs-137	4.836	0.15%	1.25%	1.26%
	Co-60	1.872	0.15%	1.12%	1.13%
B	Eu-152	17.975	0.15%	1.53%	1.54%
C	Am-241	34.678	0.15%	1.30%	1.30%
	Eu-152	32.312	0.15%	1.31%	1.32%
D	Am-241	37.153	0.15%	1.29%	1.30%
	Eu-152	28.814	0.15%	1.31%	1.32%
E	Am-241	49.135	0.15%	1.26%	1.27%
	Co-57	15.632	0.15%	1.11%	1.12%
	Ba-133	186.733	0.15%	1.11%	1.12%
	Cs-137	30.730	0.15%	1.19%	1.20%
	Co-60	27.620	0.15%	1.24%	1.25%

The uncertainties of the individual rod activities are listed in the original calibration certificates for each source set at the 99% confidence level, or approximately 2.58 standard deviations. For convenience of analysis, these values have all been converted here to the equivalent one standard deviation values. The total uncertainties per rod are typically around $\sigma_{\text{tot}} = 1.36\%$; the total fractional uncertainties for the combined sets are somewhat lower due to some smoothing of the random components.

In order to evaluate the uncertainties in the summed activities of the sets, it is necessary to distinguish between the systematic and statistical errors of the certified activities. Systematic errors are errors due to factors that globally affect all rods in a set in the same way. These may include, for example, the uncertainty in the activity of the master solution from which all of the rods were prepared or a bias in the factory calibration measurement procedure. Statistical errors refer to random factors that produce rod-to-rod variation within a set, including counting (Poisson) errors in the vendor's factory calibration measurement or variations in the amount of master solution measured into each rod.

When combining multiple rod activities, the systematic errors on the individual rods will be added directly to yield the combined systematic uncertainty while the combined statistical uncertainty is obtained by the quadrature sum of the individual statistical errors. This is a subtlety that is crucial to the correct propagation of errors in our analysis; when combining multiple rod activities the statistical parts of the errors are reduced, as a percentage of the total activity, by a factor of one over the square root of the number of rods. Thus, the systematic errors dominate the total activity uncertainty. If, instead, the total errors were simply treated as random uncertainties, and added entirely in quadrature, the expected final uncertainties would be significantly underestimated.

Only the certificate of one rod source set, set B, lists statistical errors ($\sigma_{\text{stat}} = 0.37\%$) and systematic errors ($\sigma_{\text{syst}} = 1.53\%$) separately. This value for the statistical error on each rod was used as an estimate of the statistical errors for all the other rod sets. This was considered to be a reasonable assumption, but in the end our conclusions do not depend strongly upon this approximation. The systematic error for each rod in the other sets was then estimated from the certificate total error as

$$\sigma_{\text{syst}} = \sqrt{\sigma_{\text{tot}}^2 - \sigma_{\text{stat}}^2}. \quad (\text{Eq. 1})$$

For each set, the absolute statistical errors on the individual rod activities were added in quadrature to give the statistical error on the combined activity of the set while the absolute systematic errors for each rod are propagated directly to get the combined systematic error. The combined statistical error was then added in quadrature with the combined systematic error for each rod set to obtain the total error for the set.

The combined activities for each rod set were decay corrected from the certificate reference date to the date of measurement. The uncertainties listed for the final decay corrected activities also include the small uncertainties associated with the nuclide half-lives.

Measurement Geometry and Apparatus

The rod source comparison measurements were performed in a geometry that is typical of systems designed to assay 208 liter drums, and for which similar rod sources are often used both in calibration and verification measurements. The measurements were performed on a TGS/SGS system [2], operated in SGS mode. A 120% relative efficiency coaxial HPGe detector was used.

For each set, six rods were placed in an empty 208 liter drum, each oriented parallel to the drum's axis at a different radial distance. The rods were held in place with the aid of a jig designed for use in the calibration of SGS systems, shown in Figure 1. The six radial positions selected were designed such that when the drum is rotated each rod sweeps out a cylindrical shell at the center of an annular region of equal volume. The jig also allows three additional rod positions, which were not used in these measurements. The radii of all available jig positions are listed in Table II. This configuration is used in calibration measurements to simulate a uniform source distribution [1]. It is not possible in this measurement to check the activities of individual rods, or to test for possible axial nonuniformities in the source distributions.

For each measurement the drum was placed on the turntable platform and rotated at constant speed of 4 rpm. In SGS mode, continuous measurements of a rotating drum are made with the detector platform in each of several vertical positions or segments. For these measurements, only a single segment was used, with the detector at a height corresponding to the approximate the mid height of the drum. Measurements were made for a fixed live-time of 3,600 seconds (1 hour) with the 20.32 cm (8") by 10.16 cm (4")

collimator fully open. The identical geometry was used in all the measurements. Each rod-source measurement was preceded by a measurement of the ambient background.

ANALYSIS

All measurements were analyzed using Genie 2000 Gamma Acquisition & Analysis (GAA) software [3]. For each measurement, a normalized background was stripped from the spectrum, and peak areas were determined for each gamma energy listed in the certificate using an interactive, non-linear least squares fitting procedure.

Table II Radial positions available in rod source jig for waste assay calibrations using 208 liter drum. Positions not used in this measurement are shown grayed out.

Position 1	Radius = 0.0 cm
Position 2	Radius = 5.9 cm
Position 3	Radius = 14.3 cm
Position 4	Radius = 18.3 cm
Position 5	Radius = 21.7 cm
Position 6	Radius = 24.7 cm
Position 7	Radius = 25.5 cm
Position 8	Radius = 26.2 cm
Position 9	Radius = 27.3 cm

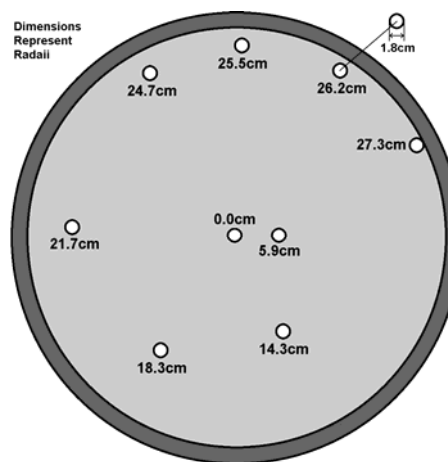


Figure 1 Diagram showing the layout of rod positions in the 208-liter Drum Calibration Jig

Efficiency Calibration

In order to perform the comparison, one of the rod-source sets (D) was selected to serve as a reference. This mixed Am-241 and Eu-152 set covers a sufficiently broad range of energy that all of the gamma energies from the other measured sets fall within the span of the efficiency calibration points. The combined source certificate data for this rod set is listed in Table VII of Appendix A.

Efficiency calibration data points were created by comparing the measured peak area data for rod set D with the expected gammas-per-second count rate derived from the source certificate. These are listed in Appendix A. An efficiency calibration function of the “linear” type was created for the measurement geometry using the GAA software. This function has the form

$$\log(\varepsilon) = p_1 \cdot E + p_0 + p_{-1} \cdot E^{-1} + p_{-2} \cdot E^{-2} + p_{-3} \cdot E^{-3}, \quad (\text{Eq. 2})$$

where ε is the efficiency (counts/ γ), E is the energy in keV, and the p_n are parameters determined by a linear least-squares fit to the efficiency data points. The coefficients of this fit are listed in Table IX of Appendix A and the efficiency function is plotted in Figure 2. Although efficiency curves are typically plotted in logarithmic scale to make the linearity of the efficiency obvious, this also has the effect of visually suppressing the error bars and residuals associated with the data points. Because of this, the calibration fit is plotted here in linear scale in order to emphasize the quality of the fit to the data.

The calibration measurement data were then reanalyzed using the calibration curve as a self consistency check. The Am-241 activity, measured at a single gamma energy, is calculated at 0.994 ± 0.038 times the certificate value. The Eu-152 activity was calculated separately for each of the eight gamma lines measured, and a weighted average activity was calculated for the nuclide. The weighted average activity was 1.0004 ± 0.008 times the certificate activity. These results confirm the quality of the calibration fit. Table X in Appendix A provides a line-by-line comparison of the results.

The reference rod set was re-measured with the ordering of the rods in the jig reversed in order to evaluate the effects of possible rod-to-rod variations on the experiment. Differences in the measured activity of the set were found to be small and in keeping with the claimed statistical uncertainties.

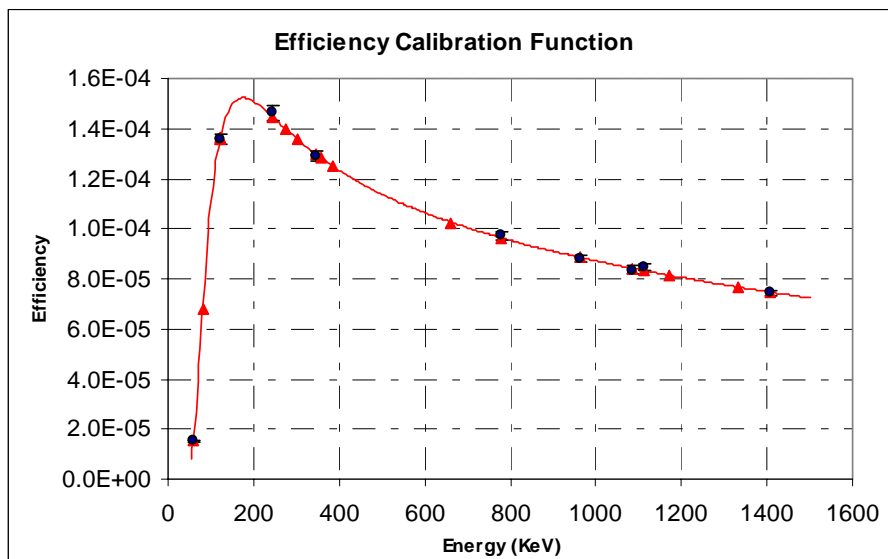


Figure 2. Efficiency calibration curve based on rod set D. Blue points are the actual measured efficiency data points, while red triangles indicate all energies of interest in this series of measurements.

MEASUREMENT RESULTS

All rod sets were measured in an identical geometry to that of the calibration measurement. The activity, A , in μCi , at each gamma line in the spectrum is calculated from the peak area as

$$A = \frac{N}{Y \cdot t \cdot \varepsilon} \times \frac{1}{37,000} \quad , \quad (\text{Eq. 3})$$

where N is the net number of counts (peak area), Y is the yield (branching ratio) of the gamma ray, t is the measurement live time, ε is the efficiency and $1/37,000$ is the conversion factor from decays per second to μCi .

The percent error in activity is given by

$$\left(\frac{\sigma_A}{A} \right)^2 = \left(\frac{\sigma_N}{N} \right)^2 + \left(\frac{\sigma_\varepsilon}{\varepsilon} \right)^2 \quad , \quad (\text{Eq. 4})$$

where we make the approximation that the uncertainties on the gamma yield and live counting time are negligible. The uncertainty in the number of counts, N , per peak is obtained from the least squares fitting procedure performed by the Genie 2000 software, and is in general larger than the simple Poisson counting error $\sigma_N = \sqrt{N}$, as it includes additional uncertainty due to the background estimation. The uncertainty in the efficiency calibration is also calculated by Genie 2000, which propagates the errors in the calibration fit parameters.

Nuclide to nuclide activities within a single rod set can vary by more than an order of magnitude. In order to compare results across nuclides, it is convenient to consider the ratio, R , of the measured activity A to certificate activity, a :

$$R = \frac{A}{a} \quad (\text{Eq. 5})$$

The uncertainty is

$$\sigma_R = \sqrt{\left(\frac{\sigma_A}{A}\right)^2 + \left(\frac{\sigma_a}{a}\right)^2} \cdot R. \quad (\text{Eq. 5})$$

These ratios are plotted by energy in Figure 3 for each rod set measured, and further broken down by nuclide within each rod set. The detailed measurement and certificate data for each set is tabulated in Appendix B.

The Eu-152 sources exhibit excellent uniformity across the full range of energies and the activity ratios are seen to be consistent with unity within the total experimental errors. However, the multi-nuclide rod sets show variability from nuclide to nuclide in excess of that expected from the calculated uncertainties.

We note that Rod Set A has a trend of increasing relative activity toward low energy, observed in the nuclides Ba-133 and Am-241. At first glance this looks like a miscalculation of attenuation effects resulting from minor differences in manufacture between Rod Set A and the calibration set, Rod Set D. In fact, the trend observed in the four highest Ba-133 lines is due to difficulties in estimating the background continua beneath the closely spaced group of peaks, which produces a slight systematic discrepancy in the peak area estimates for the nuclide. The identical effect is observed in Rod Set E, but in this case the low activity ratios observed for the nearby 122 keV Co-57 and 59 keV Am-241 lines rule out its attribution to attenuation effects. Furthermore, Rod Set E is of identical construction to calibration Rod Set D.

The lowest energy Ba-133 peak is seen to have the highest measured activity ratio for the nuclide in both rod sets. This peak coincides with the region of steepest increase in the calibration curve, as shown in Figure 2, where the function is most sensitive to small uncertainties in the fit parameters. This is reflected in the large error bar shown in both graphs; in both cases the measured activity at this peak is experimentally consistent with the other peaks for the nuclide.

We are left with the conclusion that the observed high relative activity for Am-241 in Rod Set A is real, and that despite the line-by-line variation in Ba-133, the weighted mean activity for all lines of the nuclide should be accurate within the estimated uncertainties.

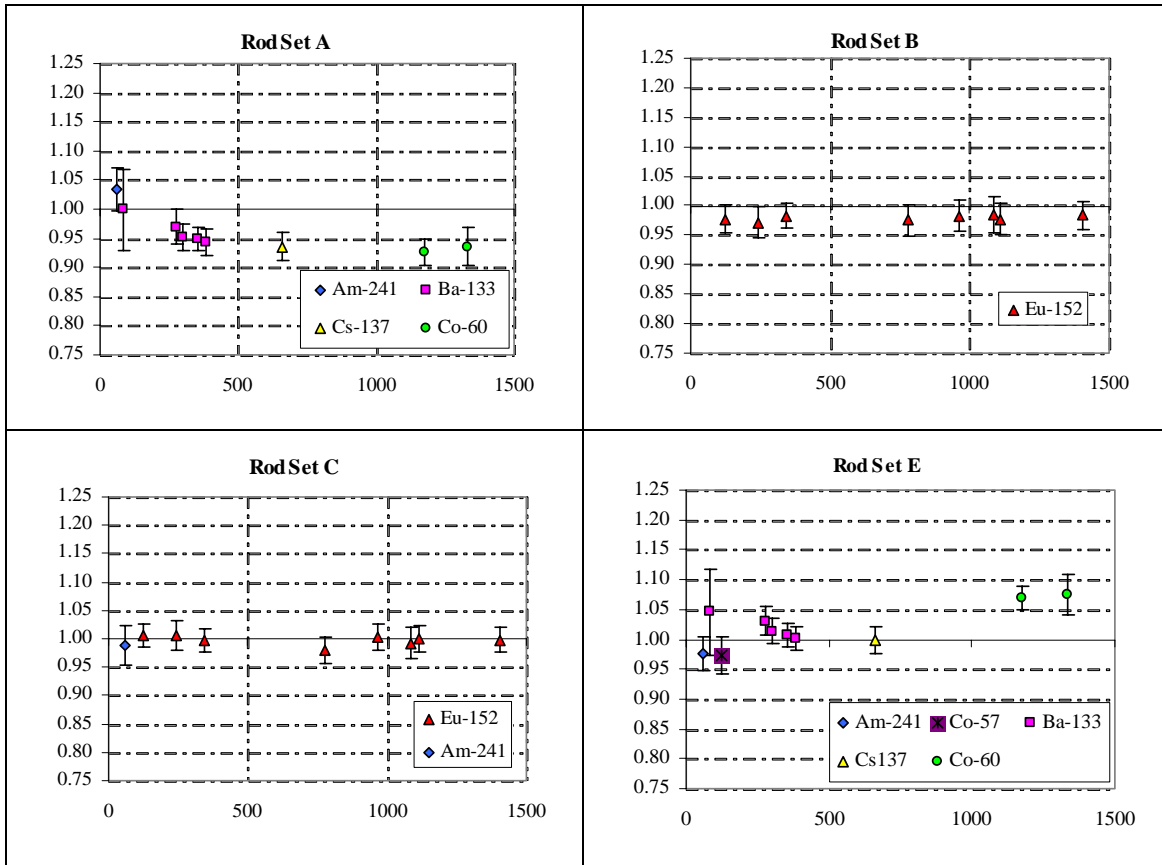


Figure 3 Ratios of measured to certificate activities calculated line-by-line for each rod set. The horizontal axis of each plot is the peak energy in keV.

Weighted Mean Nuclide Activities

The weighted mean activity for each nuclide is calculated as

$$\langle A \rangle = \frac{\sum_{\text{lines}} \frac{A}{\sigma_A^2}}{\sum_{\text{lines}} \frac{1}{\sigma_A^2}}, \quad (\text{Eq. 7})$$

where the sums are over all lines for that nuclide. The error on the mean activity is

$$\sigma_{\langle A \rangle} = \left(\sum_{\text{lines}} \frac{1}{\sigma_A^2} \right)^{-1/2}. \quad (\text{Eq. 8})$$

As in the single-line analyses, it is preferable to work with ratios of activities. The ratios and uncertainties are again calculated using equations (5) and (6), but with the substitutions $A \rightarrow \langle A \rangle$

and $\sigma_A \rightarrow \sigma_{\langle A \rangle}$. The results of these calculations for each nuclide are tabulated and briefly discussed below.

Rod Set A Results

Rod Set A contains a mixture of Am-241, Ba-133, Cs-137, and Co-60. The Am-241 activity was measured at 33.90 μCi , 1.035 \pm 0.037 times the certificate activity of 32.756 μCi . The difference is slightly less than one standard deviation of the total experimental error.

The weighted average of the five Ba-133 activities is 21.866 μCi , or 0.952 \pm 0.015 times the certificate value of 22.973. This represents a discrepancy of greater than 3σ between the certificate value and measurement, indicating an inconsistency between the Set A and Set D certificates.

The Cs-137 activity is 4.525 μCi , or 0.936 \pm 0.023 times the certificate value of 4.836 μCi , and the weighted mean of the two Co-60 points is 0.929 \pm 0.015 times the certificate value. These latter three results all represent significant discrepancies between the certificate values and measurement. These results are summarized in Table III.

Table III Rod Set A Nuclide Results Summary. Activities are in μCi .

Nuclide	Certificate	Measured	Ratio
Am-241	32.756 \pm 0.404	33.901 \pm 1.123	1.035 \pm 0.037
Ba-133	22.973 \pm 0.280	21.866 \pm 0.217	0.952 \pm 0.015
Cs-137	4.836 \pm 0.061	4.525 \pm 0.095	0.936 \pm 0.023
Co-60	1.872 \pm 0.021	1.740 \pm 0.057	0.929 \pm 0.032

Rod Set B Results

Rod Set B contains only Eu-152. The combined weighted average of the activities is 17.611 \pm 0.126 μCi . The ratio of measured to certificate values is 0.980 \pm 0.017. The measurement deviates from the certificate value by 1.21 σ . This deviation is seen to be approximately uniform across all energies, and so represents a relative bias between the Set B and Set D certificates. However, the size of the bias is reasonably consistent with the total experimental error, and therefore with the quoted certificate errors. It is therefore concluded that sets B and D are consistent.

Table IV Rod Set B Nuclide Results Summary. Activities are in μCi .

Nuclide	Certificate Activity	Measured Activity	Ratio
Eu-152	17.975 \pm 0.277	17.611 \pm 0.126	0.980 \pm 0.017

Rod Set C Results

Rod Set C contains the same nuclide mix as the calibration set, Am-241 and Eu-152. The weighted average of the Eu-152 activities is 32.25 \pm 0.214 μCi , compared to the certificate value of 32.312 \pm 0.427 μCi . The ratio of the measured to certificate values is 0.998 \pm 0.015. The Am-241 activity from the single measured data point is 0.980 \pm 0.035 times the certificate value. Both nuclide results are consistent with the certificate values within the combined experimental and certificate errors. The nuclide results are summarized in Table V.

We note that because the same gamma energies is set C are identical to the reference set, it is also possible to evaluate the activities without reliance on the efficiency calibration curve at all, by instead using the efficiency data points listed in Table VIII of Appendix A directly. This slightly reduces the experimental errors by eliminating the small uncertainties in the calibration fit parameters. As a check, such a direct calculation was done for this set and for set B, which contains a subset of the reference energies. The differences in the activities found by both methods are minimal, as expected based upon the small calibration errors observed in Table X. For consistency, however, all results reported in this paper utilize the calibration fit.

Table V *Rod Set C Nuclide Results Summary. Activities are in μCi .*

Nuclide	Certificate Activity	Measured Activity	Ratio
Am-241	34.678 ± 0.452	34.255 ± 1.135	0.988 ± 0.035
Eu-152	32.312 ± 0.427	32.255 ± 0.214	0.998 ± 0.015

Rod Set E Results

Rod Set E contains Am-241, Co-57, Ba-133, Cs-137, and Co-60. The Co-60 activity was found to be significantly higher than the certificate value, with a measured value 1.070 ± 0.019 times the expected value of $27.620 \mu\text{Ci}$, a disagreement of more than 3σ . The other nuclides are found to be within 1σ of the certificate values. The nuclide results are summarized in Table VI.

Table VI *Rod Set E Nuclide Results Summary. Activities are in μCi .*

Nuclide	Certificate Activity	Measured Activity	Ratio
Am-241	49.135 ± 0.625	47.948 ± 1.274	0.976 ± 0.029
Co-57	15.632 ± 0.175	15.207 ± 0.446	0.973 ± 0.031
Ba-133	186.733 ± 2.099	188.777 ± 1.646	1.011 ± 0.014
Cs-137	30.730 ± 0.369	30.715 ± 0.597	0.999 ± 0.023
Co-60	27.620 ± 0.345	29.561 ± 0.391	1.070 ± 0.019

Discussion of Results

In order to understand the significance of the observed disparity between measured and certificate activities among the five rod source sets, consider the relative deviations of the weighted mean measured activities from the certificate values. Expressed in units of the total experimental error, this is found by

$$\Delta = \frac{(R-1)}{\sigma_R}. \quad (\text{Eq. 9})$$

This metric expresses, for each measured nuclide, by how many standard deviations the measured values disagree with the expected activities. If all certificate activities were correct and the uncertainties were within the claimed uncertainties for all nuclides, Δ should be roughly Gaussian distributed about a mean value of 0, with a standard deviation of 1.

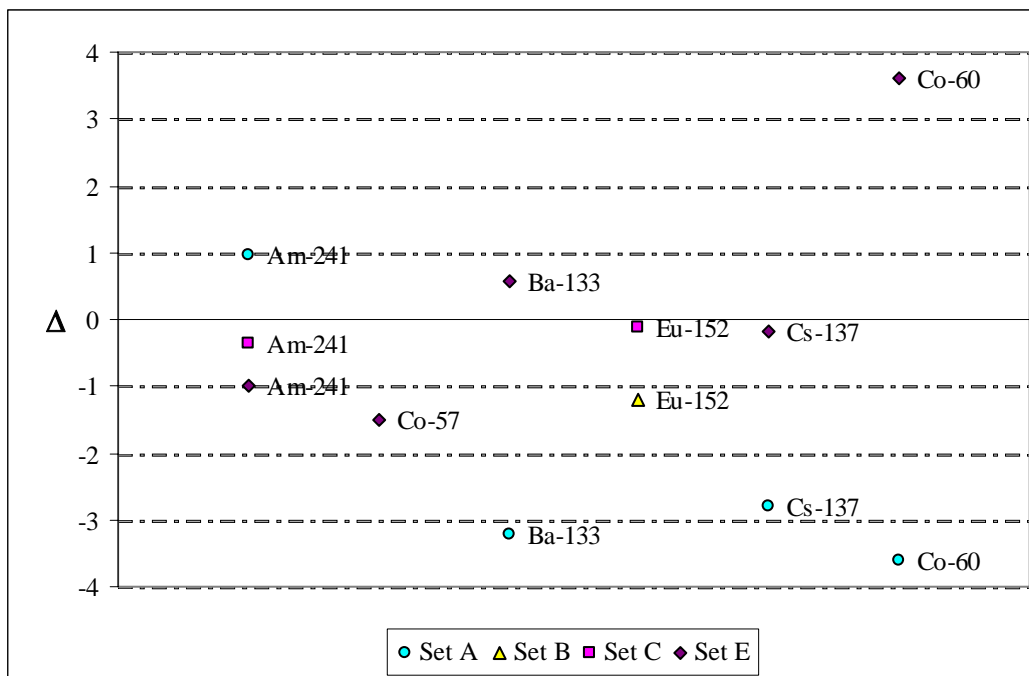


Figure 4 For each nuclide in each rod set, the difference from unity of the ratio of measured to certified activities is plotted in units of the total experimental error.

The values obtained for all nuclides in the four rod source sets are plotted in Figure 4. The distribution has a clearly noticeable offset; the mean value is -0.74. The spread of values is also much wider than expected; approximately two-thirds of the data should fall within ± 1 , but in fact less than half do. One fourth of the data set lies outside of three experimental errors from the expected value. The standard deviation of the data points themselves is 1.91 experimental errors. This is a clear indicator that the total errors are underestimated.

Two of the rod sets, B and C, are in agreement with the calibration set D to within the experimental errors. This consistency suggests that these three independent rod sets are accurately calibrated, that the activity uncertainties of these sources are reasonably estimated, and that we have properly estimated the experimental uncertainties.

The wide spread of the data from the remaining rod sets indicates that the certificate uncertainties overstate the precision with which the rods have been calibrated. Rods A and E exhibit overall biases and internal, nuclide to nuclide inconsistencies that are in excess of the claimed precision.

CONCLUSION

We have found that calibrating a waste assay system using one of these source sets could introduce significant errors in waste assay results, on the order of 5% or more. In particular, the internal discrepancies in the multi-nuclide sets can skew the calibration fit, resulting in energy dependent systematic errors which can be difficult to detect. These findings lead us to conclude that, where possible, the certified activities and associated uncertainties on newly acquired sources should be independently confirmed before relying on them as calibration standards.

REFERENCES

1. S. Croft, R.D. McElroy, “The Calibration of Segmented Gamma Scanners Using Rod Sources”, Proceedings WM '05, February 27-March 3, 2005 Tucson, Arizona, USA
2. R. Venkataraman, *et al*, “An Integrated Tomographic Gamma Scanning System for Non Destructive Assay of Radioactive Waste”, paper presented at the XI Symposium of Radiation Measurements and Applications, Ann Arbor, Michigan, USA, May 22-25, 2006 (to be published in a special edition of Nuclear Instruments and Methods in Physics Research A).
3. Canberra Industries, Inc. *Genie 2000 Customization Tools Manual*. Meriden, CT (2004).

APPENDIX A – TABULATED CALIBRATION DATA

Table VII Calibration source certificate data for combined rod set D, used as reference source.

Nuclide	E (keV)	Activity (μCi)	Rel. Unc.	Yield	γ/s
Am-241	59.540	37.153	1.30%	0.363	499006 \pm 6487
Eu-152	121.78	28.814	1.32%	0.284	302778 \pm 3992
	244.690	28.814	1.32%	0.075	79852 \pm 1053
	344.27	28.814	1.32%	0.265	282522 \pm 3724
	778.89	28.814	1.32%	0.127	135824 \pm 1791
	964.01	28.814	1.32%	0.144	153521 \pm 2024
	1085.780	28.814	1.32%	0.100	106612 \pm 1405
	1112.020	28.814	1.32%	0.133	141794 \pm 1869
	1407.95	28.814	1.32%	0.207	220687 \pm 2909

Table VIII Calibration measurement data: peak areas, count rates and efficiencies with corresponding uncertainties.

Nuclide	E (keV)	Peak Area N	N/s	Rel. Unc.	Efficiency	Rel. Unc.
Am-241	59.540	27548.88 \pm 578.5	7.65	2.10%	1.534E-05	2.47%
Eu-152	121.78	148074.31 \pm 992.1	41.13	0.67%	1.358E-04	1.48%
	244.690	42056.98 \pm 761.2	11.68	1.81%	1.463E-04	2.24%
	344.27	131323.75 \pm 748.5	36.48	0.57%	1.291E-04	1.44%
	778.89	47651.73 \pm 533.7	13.24	1.12%	9.745E-05	1.73%
	964.01	48782.81 \pm 502.5	13.55	1.03%	8.827E-05	1.67%
	1085.780	32057.35 \pm 452.0	8.90	1.41%	8.353E-05	1.93%
	1112.020	43332.33 \pm 494.0	12.04	1.14%	8.489E-05	1.74%
	1407.95	59133.56 \pm 484.9	16.43	0.82%	7.443E-05	1.55%

Table IX Efficiency calibration parameters

p_1	-1.169E-04
p_0	-4.014E+00
p_{-1}	7.784E+01
p_{-2}	-6.725E+03
p_{-3}	-4.313E+04

Table X Comparison of certificate activity values and re-analysis results of calibration data using calibration curve. Activities are given in μCi .

Nuclide	Energy	Certificate	Re-Analysis	% Difference
Am-241	59.540	37.153	36.932	-0.60%
Eu-152	121.78	28.812	28.767	-0.16%
	244.690	28.812	28.903	0.32%
	344.27	28.812	28.769	-0.15%
	778.89	28.812	28.887	0.26%
	964.01	28.812	28.523	-1.00%
	1085.780	28.812	28.861	0.17%
	1112.020	28.812	29.167	1.23%
	1407.95	28.812	28.712	-0.35%

APPENDIX B – TABULATED MEASUREMENT DATA

Table XI Measurement data for rod set A: Certificate activities for all nuclides, measured peak areas and uncertainties.

Certificate Data					Peak Data	Calibration		Results
Nuclide	E (keV)	Activity (μCi)	Rel. Unc.	Yield	Area	Eff.	%Err	Activity (μCi)
Am-241	59.540	32.756	1.23%	0.363	2.51E+04 \pm 548	1.53E-05	2.49%	33.90 \pm 1.123
Ba-133	81.000	22.973	1.22%	0.330	6.84E+04 \pm 267	6.78E-05	6.75%	22.94 \pm 1.551
	276.397	22.973	1.22%	0.069	2.86E+04 \pm 560	1.40E-04	1.96%	22.27 \pm 0.617
	302.839	22.973	1.22%	0.178	7.04E+04 \pm 576	1.36E-04	1.79%	21.87 \pm 0.430
	356.005	22.973	1.22%	0.600	2.24E+05 \pm 825	1.29E-04	1.60%	21.81 \pm 0.359
	383.850	22.973	1.22%	0.087	3.14E+04 \pm 409	1.25E-04	1.60%	21.65 \pm 0.447
Cs-137	661.650	4.836	1.26%	0.851	5.26E+04 \pm 466	1.03E-04	1.91%	4.53 \pm 0.095
Co-60	1173.216	1.872	1.13%	1.000	1.88E+04 \pm 291	8.13E-05	1.44%	1.74 \pm 0.037
	1332.486	1.872	1.13%	1.000	1.79E+04 \pm 286	7.67E-05	2.86%	1.75 \pm 0.057

Table XII Measurement data for rod set B: Certificate activities for all nuclides, measured peak areas and uncertainties.

Certificate Data					Peak Data	Calibration		Results
Nuclide	E (keV)	Activity (μCi)	Rel. Unc.	Yield	Area	Eff	Rel. Unc.	Activity (μCi)
Eu-152	121.780	17.975	1.54%	0.284	9.03E+04 \pm 766	1.358E-04	1.48%	17.572 \pm 0.300
	244.690	17.975	1.54%	0.075	2.55E+04 \pm 171	1.463E-04	2.24%	17.471 \pm 0.408
	344.270	17.975	1.54%	0.265	8.05E+04 \pm 544	1.291E-04	1.44%	17.663 \pm 0.280
	778.890	17.975	1.54%	0.127	2.90E+04 \pm 420	9.745E-05	1.73%	17.536 \pm 0.396
	964.010	17.975	1.54%	0.144	2.99E+04 \pm 412	8.827E-05	1.67%	17.661 \pm 0.383
	1085.780	17.975	1.54%	0.100	1.97E+04 \pm 371	8.353E-05	1.93%	17.707 \pm 0.478
	1112.020	17.975	1.54%	0.133	2.64E+04 \pm 380	8.489E-05	1.74%	17.555 \pm 0.397
	1407.950	17.975	1.54%	0.207	3.63E+04 \pm 382	7.443E-05	1.55%	17.688 \pm 0.332

Table XIII Measurement data for rod set B: Certificate activities for all nuclides, measured peak areas and uncertainties.

Certificate Data					Peak Data	Calibration		Results
Nuclide	E (keV)	Activity (μCi)	Rel. Unc.	Yield	Area	Eff	Rel. Unc.	Activity (μCi)
Am-241	59.54	34.678	1.30%	0.363	2.54E+04 \pm 561	1.534E-05	2.47%	34.255 \pm 1.135
Eu152	121.780	32.312	1.32%	0.284	1.67E+05 \pm 1060	1.358E-04	1.48%	32.497 \pm 0.523
	244.690	32.312	1.32%	0.075	4.74E+04 \pm 227	1.463E-04	2.24%	32.475 \pm 0.744
	344.270	32.312	1.32%	0.265	1.47E+05 \pm 784	1.291E-04	1.44%	32.254 \pm 0.494
	778.890	32.312	1.32%	0.127	5.23E+04 \pm 559	9.745E-05	1.73%	31.625 \pm 0.643
	964.010	32.312	1.32%	0.144	5.49E+04 \pm 538	8.827E-05	1.67%	32.427 \pm 0.629
	1085.780	32.312	1.32%	0.100	3.57E+04 \pm 457	8.353E-05	1.93%	32.068 \pm 0.743
	1112.020	32.312	1.32%	0.133	4.86E+04 \pm 503	8.489E-05	1.74%	32.317 \pm 0.655
	1407.950	32.312	1.32%	0.207	6.62E+04 \pm 514	7.443E-05	1.55%	32.257 \pm 0.560

Table XIV Measurement data for rod set B: Certificate activities for all nuclides, measured peak areas and uncertainties.

Certificate Data					Peak Data	Calibration		Results
nuclide	E (keV)	Activty (μCi)	Rel. Unc.	Yield	Area	Eff	Rel. Unc.	Activty (μCi)
Am-241	59.540	49.135	1.27%	0.363	3.55E+04 ± 329	1.53E-05	2.49%	47.948 ± 1.27
Co-57	122.063	15.632	1.12%	0.855	2.36E+05 ± 1725	1.36E-04	2.84%	15.207 ± 0.45
Ba-133	81.000	186.733	1.12%	0.330	5.82E+05 ± 2174	6.78E-05	6.75%	195.226 ± 13.20
	276.397	186.733	1.12%	0.069	2.47E+05 ± 1592	1.40E-04	1.96%	192.357 ± 3.96
	302.839	186.733	1.12%	0.178	6.09E+05 ± 1698	1.36E-04	1.79%	189.211 ± 3.42
	356.005	186.733	1.12%	0.600	1.93E+06 ± 2351	1.29E-04	1.60%	187.885 ± 3.02
	383.850	186.733	1.12%	0.087	2.71E+05 ± 1134	1.25E-04	1.60%	186.827 ± 3.09
Cs-137	661.650	30.730	1.20%	0.851	3.57E+05 ± 1224	1.03E-04	1.91%	30.715 ± 0.60
Co-60	1173.216	27.620	1.25%	1.000	3.20E+05 ± 1182	8.13E-05	1.44%	29.537 ± 0.44
	1332.486	27.620	1.25%	1.000	3.03E+05 ± 1096	7.67E-05	2.86%	29.655 ± 0.86